Fifth Annual Conference on Carbon Capture & Sequestration

Steps Toward Deployment

Geological Storage - Modeling

Long-term simulations of CO_2 storage in saline aquifer

Y. Le Gallo, L. Trenty, A. Michel

May 8-11, 2006 • Hilton Alexandria Mark Center • Alexandria, Virginia

CO_2 trapping mechanisms in saline aquifers

- Several trapping processes of CO_2 can exist with different characteristic times:
  - **structural trapping**: CO_2 is trapped as a dense phase according to the structural lithology of the storage
  - **capillary trapping**: CO_2 is trapped at residual gas saturation in the wake of the dense phase plume
  - **solution trapping**: CO_2 is dissolved in the liquid phase (oil or brine)
  - **mineral trapping**: CO_2 is incorporated into minerals due to chemical precipitation

Coupled processes in CO_2 geological storage

- multiphase fluid flow model in porous media:
  - permeability heterogeneities (absolute and relative)
  - pressure and temperature effects on CO_2 as a free or trapped phase (supercritical or gaseous) or dissolved within the aquifer.
  - pressure and temperature gradients both natural and induced during the injection process.
  - diffusion and dispersion within the aquifer and its geosphere (cap-rock and overburden).
  - reaction between host rock and storage fluids
  - fault and wells leakage pathways

Component conservation equations

- Mass

$$\overbrace{\frac{\partial}{\partial t}\left[\phi\left(\sum_{p=1}^{N_p}\rho_p\cdot S_p\cdot x_k^p\right)\right]}^{\text{accumulation}}+\nabla\cdot\left(\overbrace{\sum_{p=1}^{N_p}\rho_p\cdot x_k^p\cdot\vec{u}_p}^{\text{advection}}+\overbrace{\vec{J}_k^p}^{\text{diffusion/dispersion}}\right)+\underbrace{Q_k+R_k}_{\text{source/sink}}=0$$

  - well, aquifer
  - reaction

- Momentum

$$\vec{u}_p=-\frac{\overline{\overline{K}}\cdot k_{rp}}{\mu_p}\left(\vec{\nabla}P_p+\rho_p\cdot\vec{g}\right)$$

- Energy

$$\frac{\partial}{\partial t}\left[\phi\left(\sum_{p=1}^{N_p}\rho_p\cdot S_p\cdot U_p\right)\right]+\nabla\cdot\left(\sum_{p=1}^{N_p}\rho_p\cdot H_p\cdot\vec{u}_p+\vec{J}_T\right)+Q_T+R_T=0$$

Constitutive Equations

– Diffusion/dispersion

$$\overrightarrow{J_p^k} = \overbrace{-\rho_p \cdot S_p \cdot \frac{\phi \cdot D_p^k}{\overline{\overline{\tau}}} \cdot \vec{\nabla} x_p^k}^{\text{diffusion (Fick's law)}} \overbrace{+\rho_p \cdot D_t \cdot \left\|\overrightarrow{u_p}\right\| \cdot \vec{\nabla} x_p^k + \rho_p \cdot \left(D_l - D_t\right) \cdot \frac{\vec{\nabla} x_p^k \cdot \overrightarrow{u_p}}{\left\|\overrightarrow{u_p}\right\|} \cdot \overrightarrow{u_p}}^{\text{Hydrodynamic dispersion}}$$

– Heat flux (Fourier's law) $\overrightarrow{J_p^k} = -\lambda^* \cdot \vec{\nabla} T$

– Well source term

$$Q_k = \sum_i PI_i \cdot \frac{k_{rpi}}{\mu_{pi}} \cdot x_p^k \cdot \left[P_i - \left(P_{ref} + \overline{\rho_p}\, g \Delta Z\right]\right.$$

– Reaction

$$R_p^k = k_{reac}^k \, e^{-\frac{E_a}{RT}} \cdot S_{reac} \cdot \left[1 - \left(\frac{Q_p^k}{K_{eq,p}^k}\right)^n\right]$$

COORES coupling approach

- 3-D Dual-media multiphase (3 phases) fluid flow <u>compositional in all phases</u> with:
  - implicit pressure, temperature and components
  - sequential aqueous geochemical reaction coupling
  - external geomechanical coupling

Geochemical coupling

- Dual fluid approach => Consistency checks

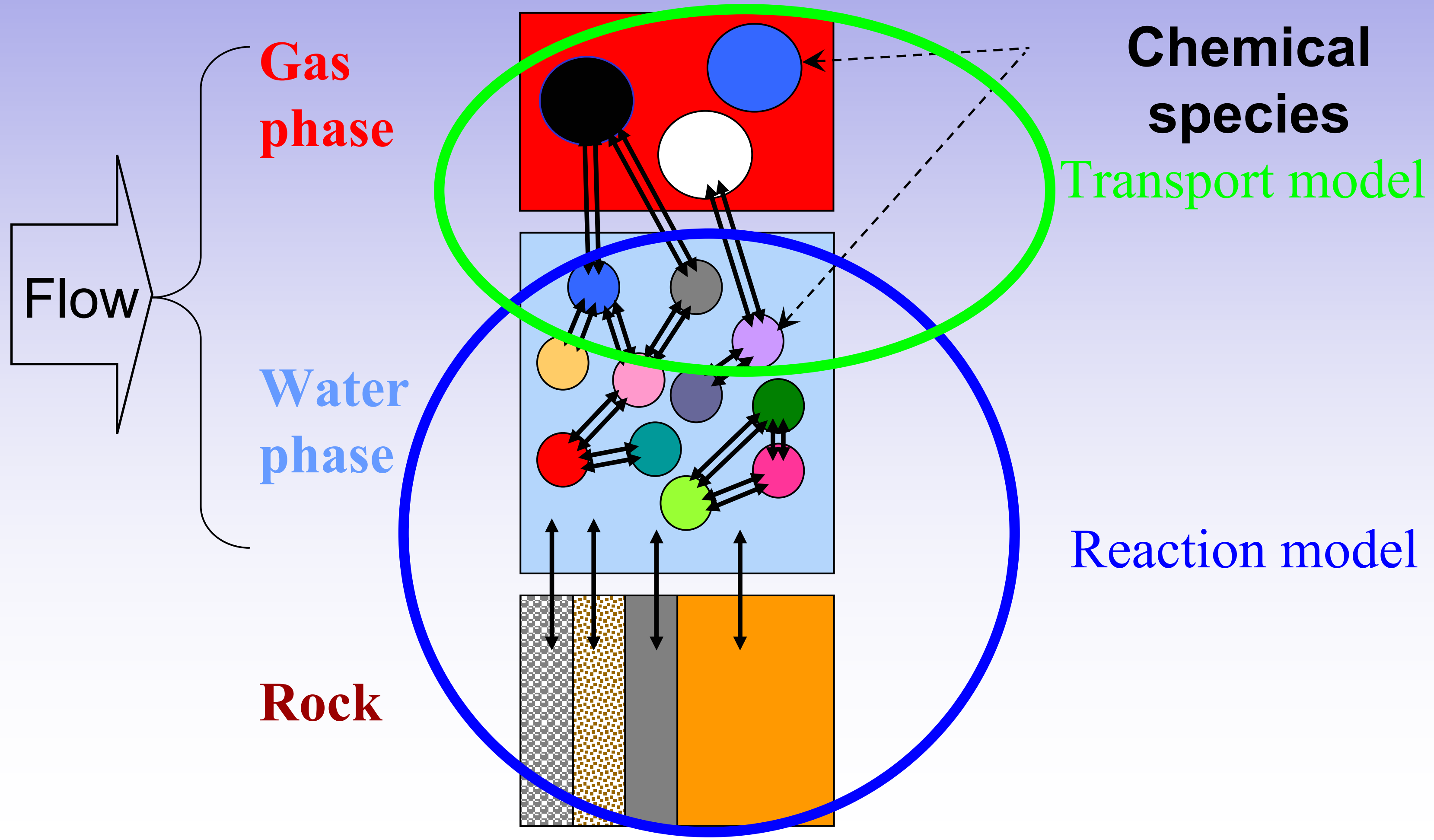

External geomechanical coupling

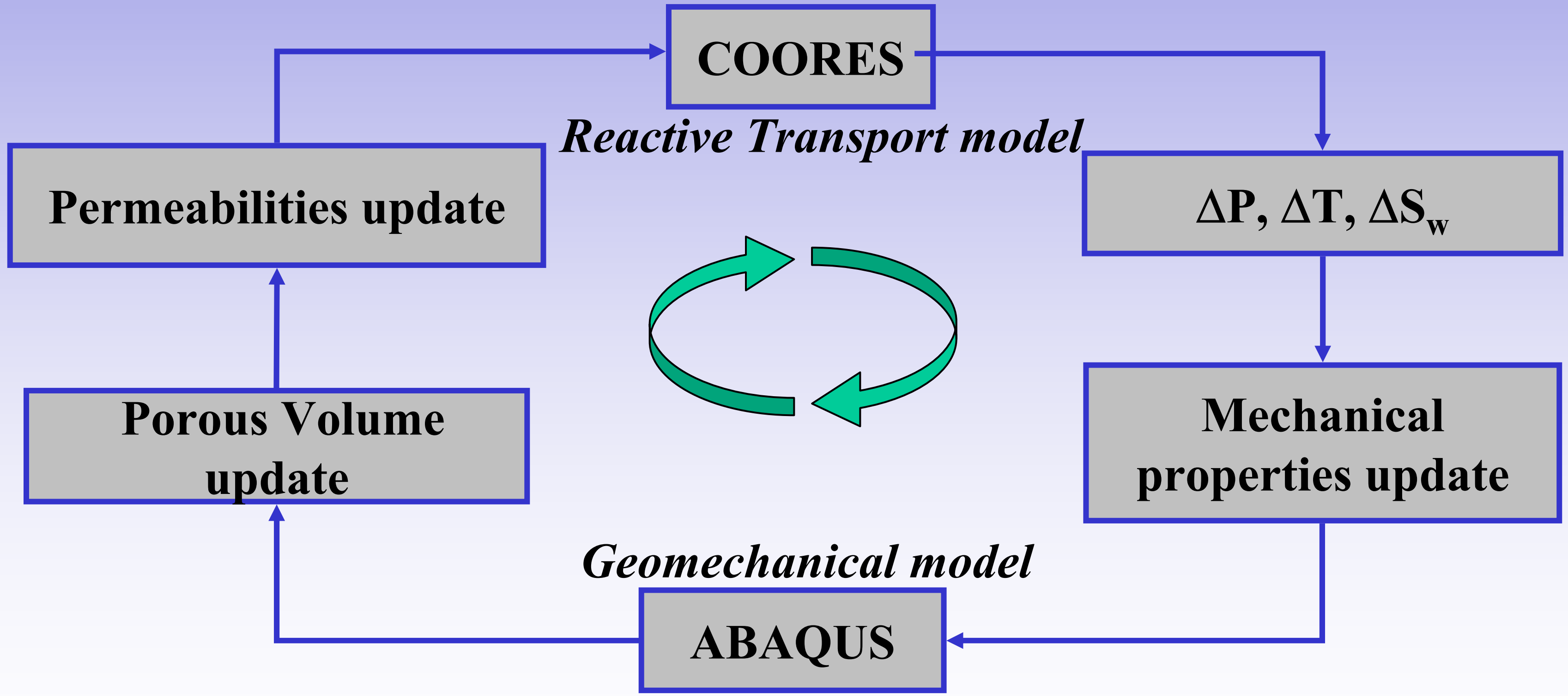

3-D CO_2 storage in an heterogeneous saline aquifer

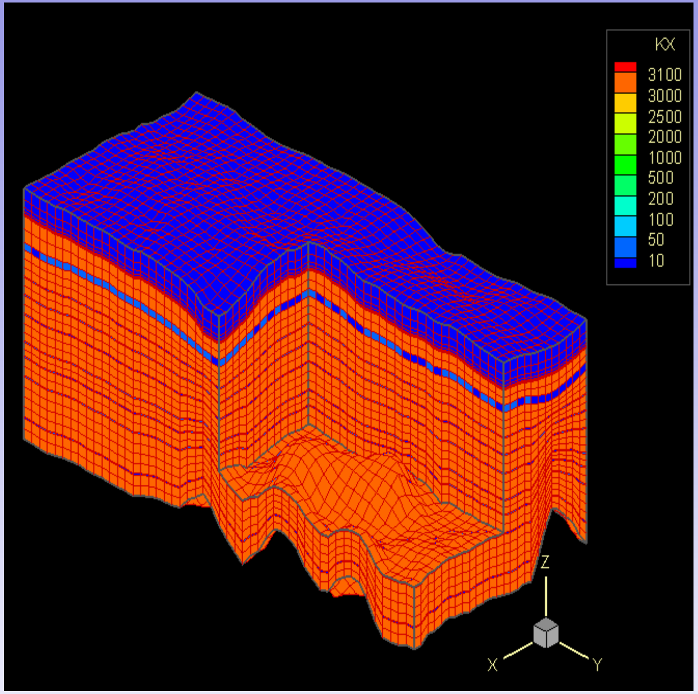

- Size: 3000 x 6000 x 260 m
  ≈ 37 500 grid blocks
- Isothermal
- Two rock types:
  - quartz rich **sand** bodies with 3000 mD permeability and 35 % porosity.
  - illite and k-feldspar rich **shale** layers with 10 mD permeability and 10 % porosity.
- Dissolution and diffusion of CO_2 in Water

Rock type mineral compositions

	sand*	shale
anorthite ($CaAl_2Si_2O_8$)	0%	10%
calcite ($CaCO_3$)	1%	10%
dolomite ($MgCa(CO_3)_2$)	1%	10%
illite ($Si_{3.43}Al_{2.24}Mg_{0.38}O_{10}(OH)_2K_{0.8}$)	3%	**25%**
k-feldspar ($KAlSi_3O_8$)	2%	**25%**
kaolinite ($Al_2Si_2O_5(OH)_4$)	2%	10%
quartz (SiO_2)	**90%**	10%

*** data from Nghiem *et al* (2004)**

Rock type relative permeabilities

- No hysteresis effect (residual trapping)

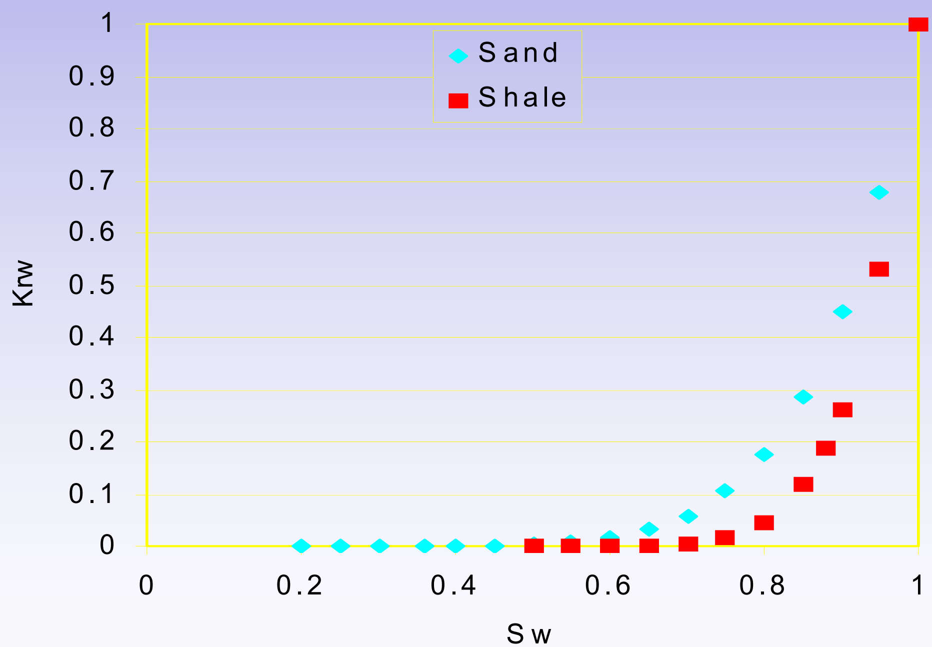

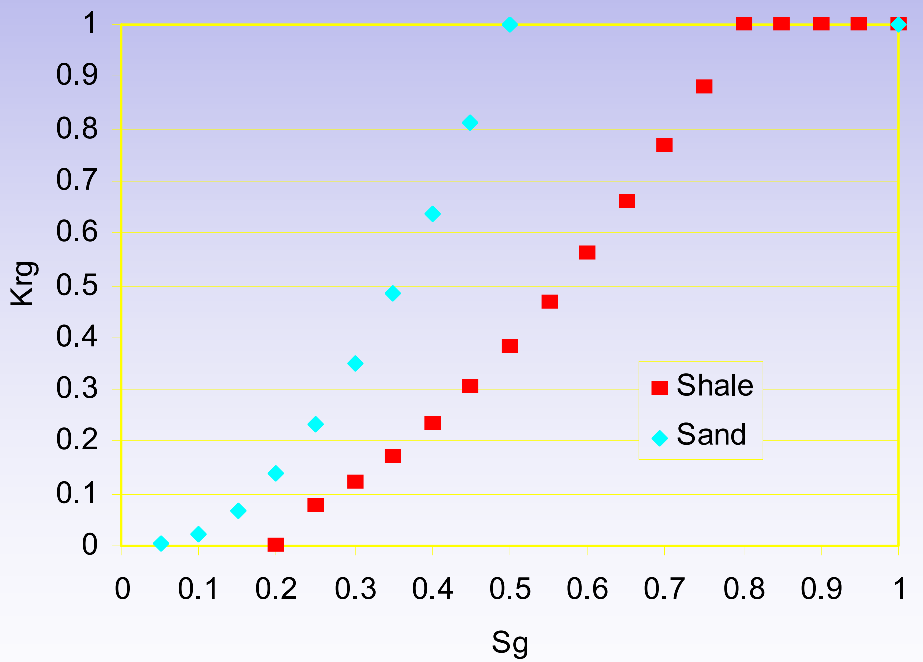

Supercritical CO_2 saturation

End of injection (50 years)

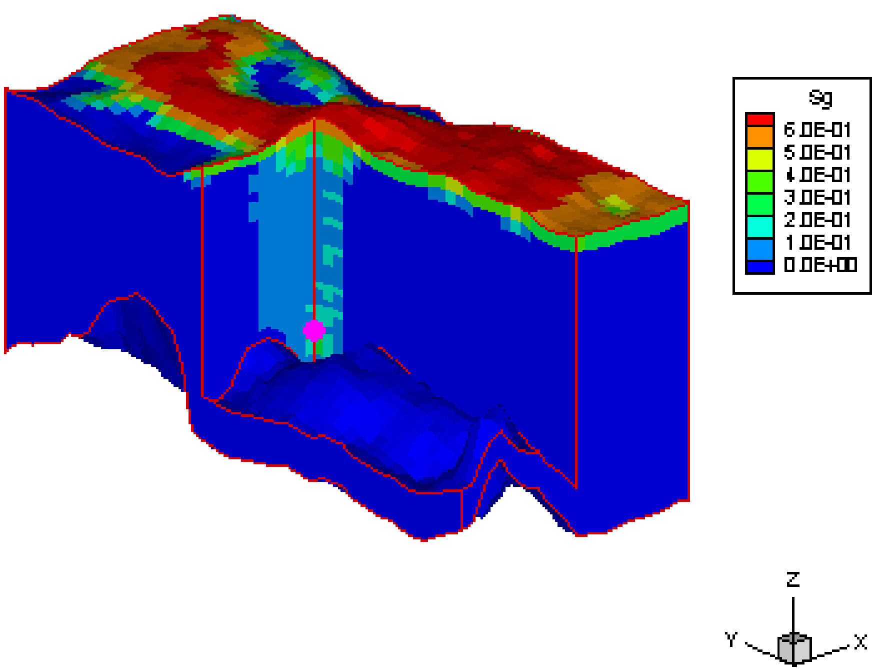

End of storage (1000 years)

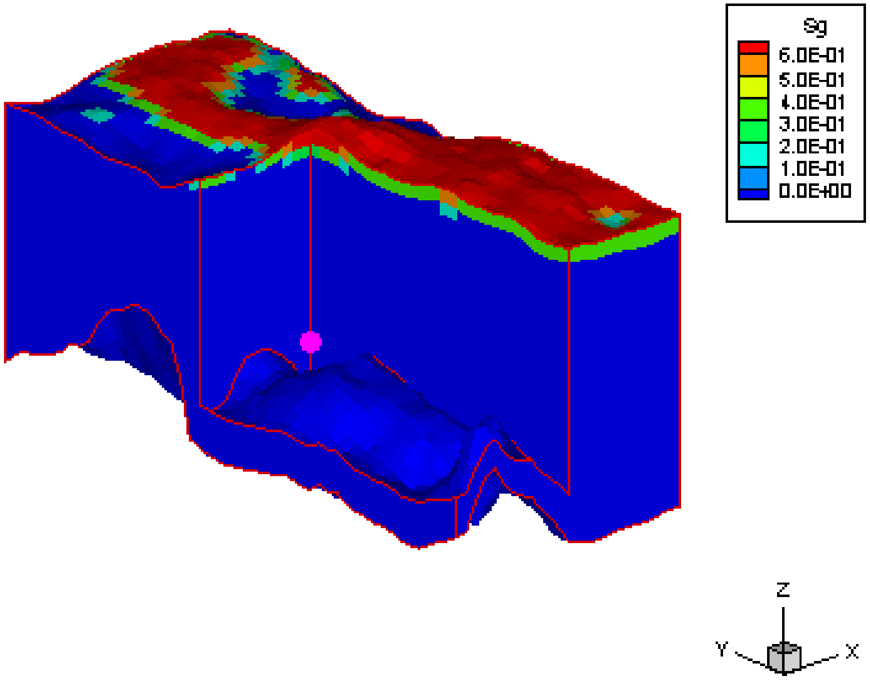

Dissolved CO_2 fraction

End of injection (50 years)

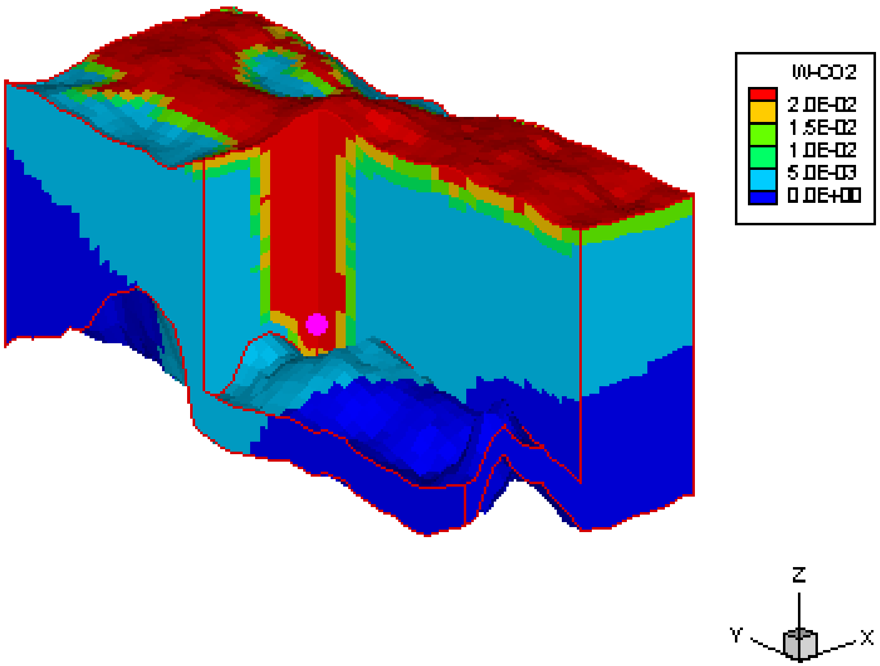

End of storage (1000 years)

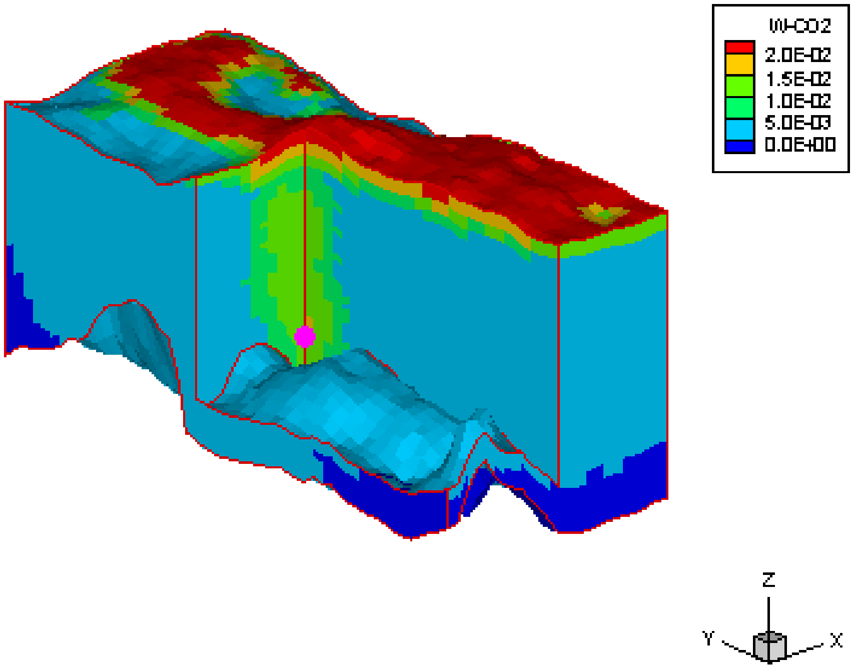

pH changes with respect to initial

End of injection (50 years)

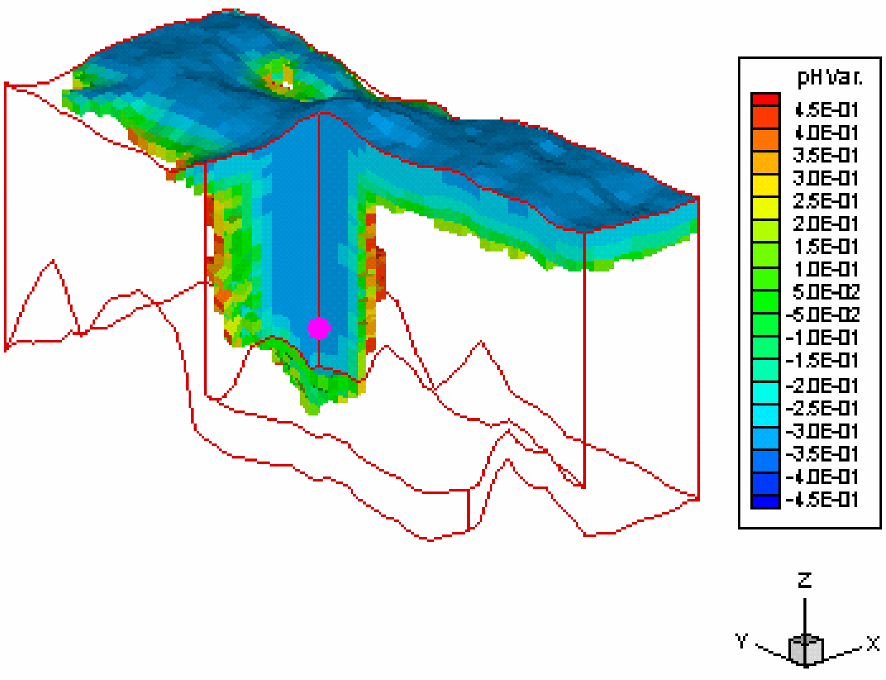

End of storage (1000 years)

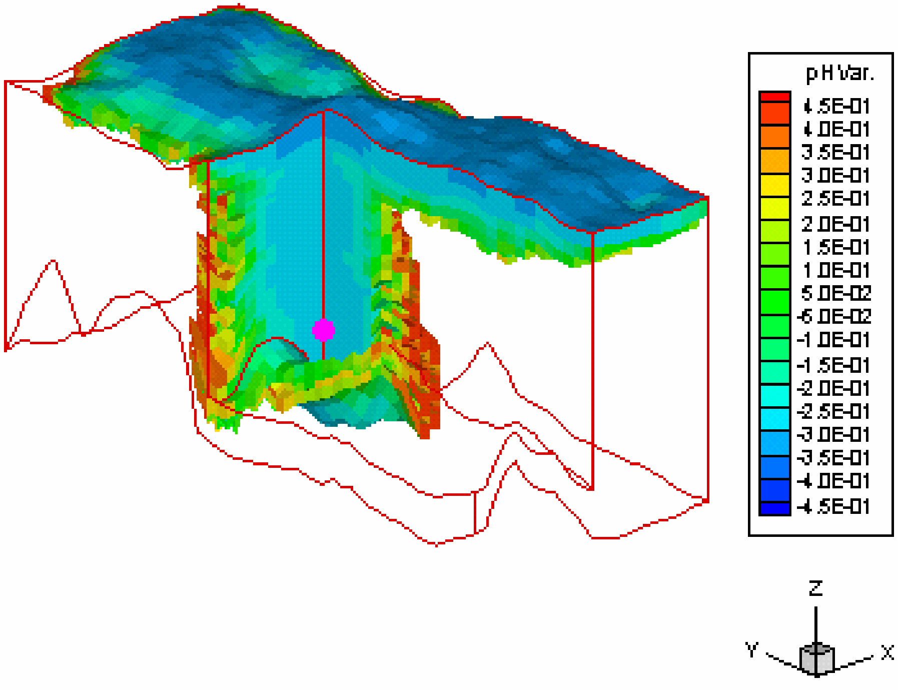

Calcite volume fraction change with respect to initial

End of injection (50 years)

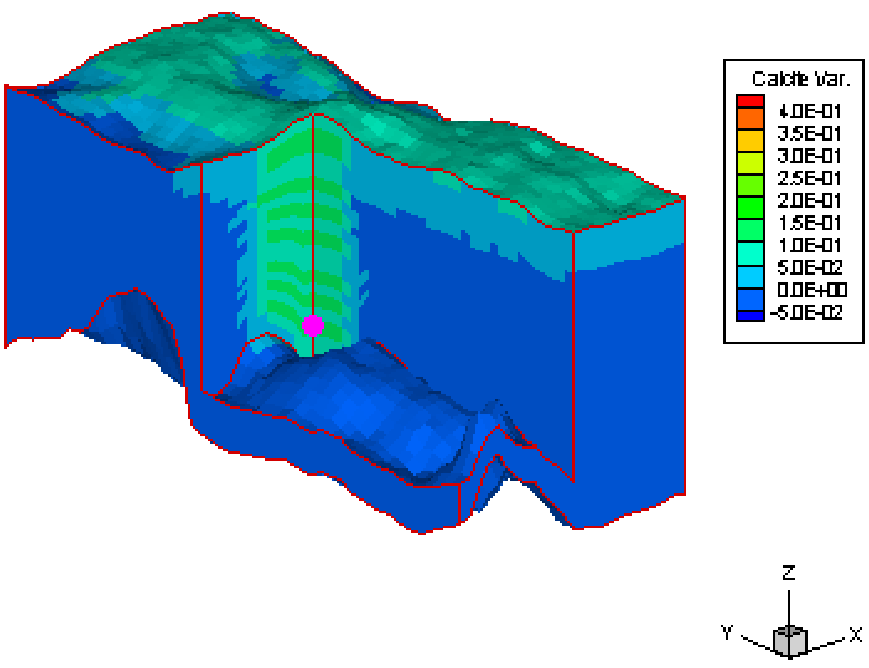

End of storage (1000 years)

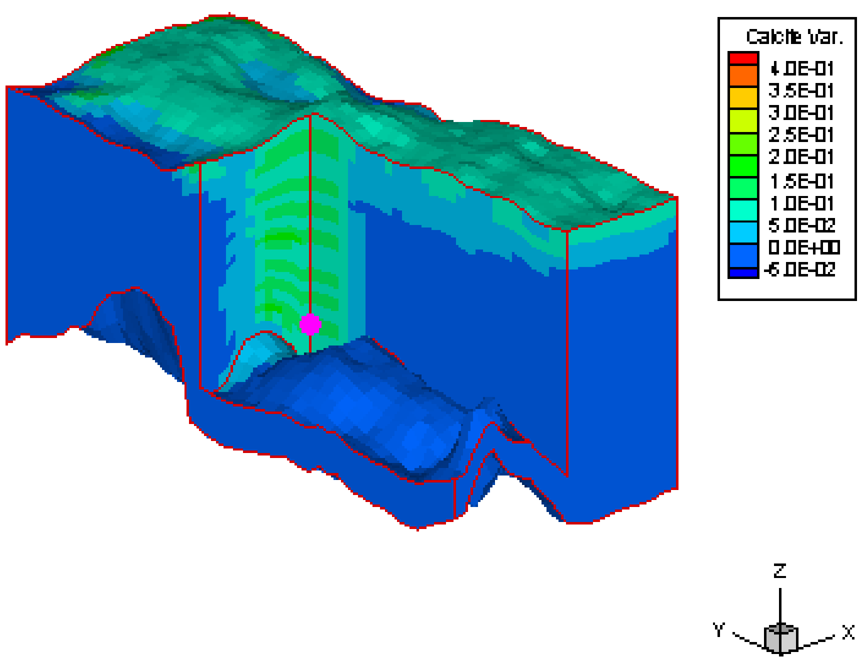

Dolomite volume fraction change with respect to initial

End of injection (50 years)

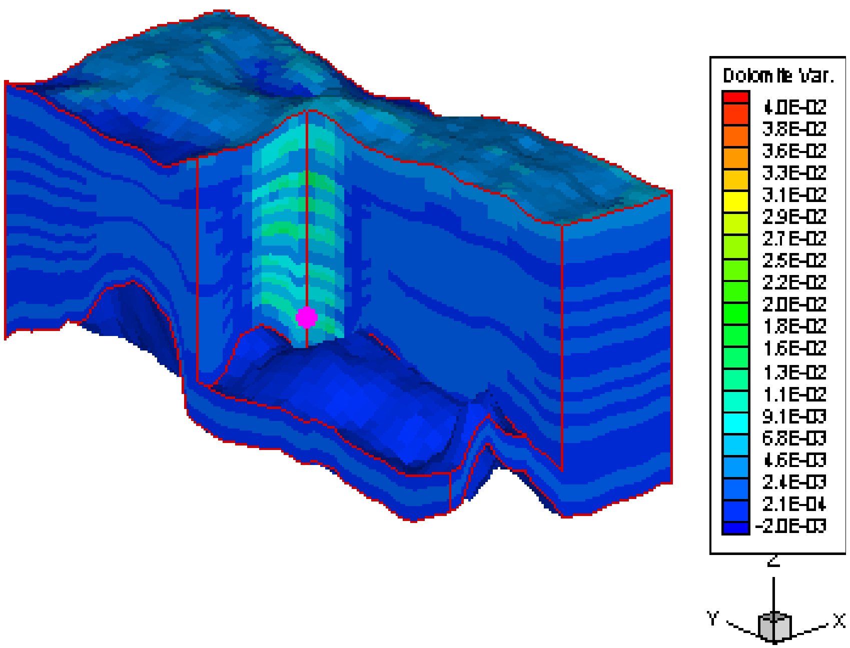

End of storage (1000 years)

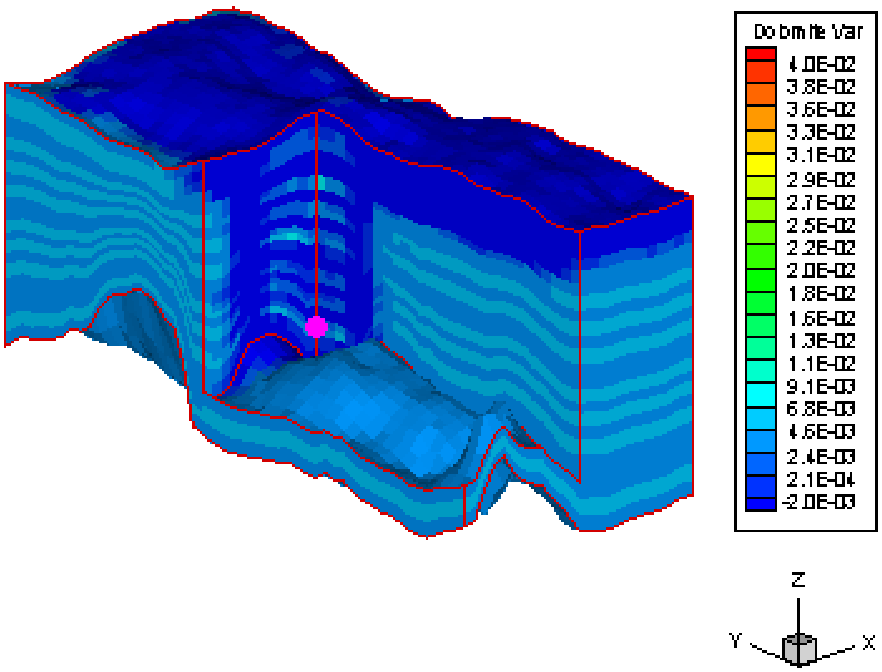

Carbonate mineral behavior during CO_2 injection

$$CO_2 + H_2O = H^+ + HCO_3^-$$

- fast kinetic rates for carbonate minerals:
- Calcite precipitation: limited by solution Ca^{2+}

$$Ca^{2+} + HCO_3^- = CaCO_3 + H^+$$

- Dolomite precipitation: limited by solution Mg^{2+}

$$Ca^{2+} + Mg^{2+} + 2HCO_3^- = MgCa(CO_3)_2 + 2H^+$$

- Parallel precipitation reactions for calcite and dolomite

K-feldspar volume fraction change with respect to initial

End of injection (50 years)

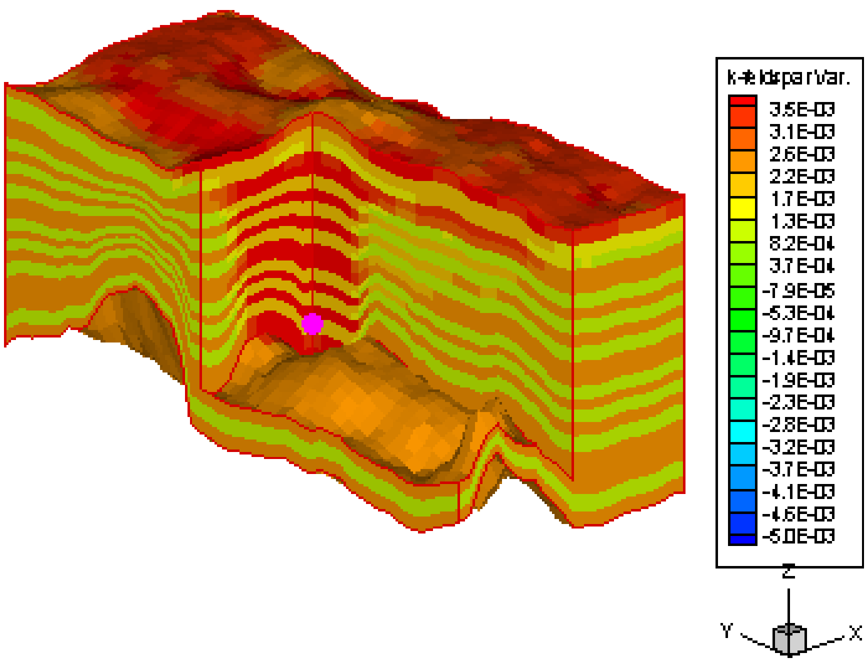

End of storage (1000 years)

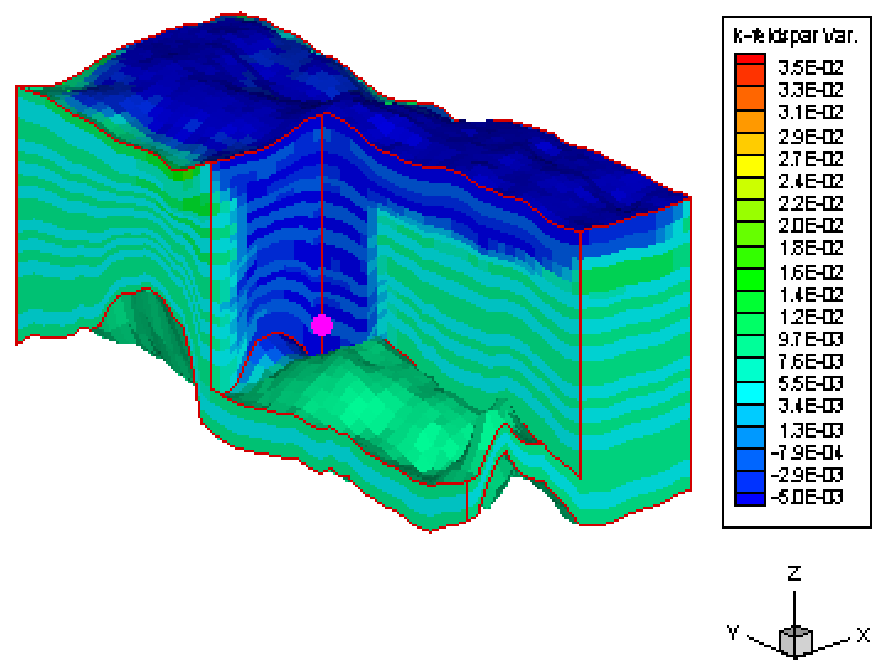

k-feldspar behavior

- during CO_2 injection:
  - k-feldspar precipitation due to higher kinetic reactivity (2 orders of magnitude) with respect to other alumino-silicates minerals (illite, kaolinite) mainly in the sand zone due to solution equilibrium between sand and shale

    $2\ H_2O + K^+ + Al^{3+} + 3\ SiO_{2(aq)} = KAlSi_3O_8 + 4H^+$
- during CO_2 storage:
  - k-feldspar dissolution due to other alumino-silicates reactions

Kaolinite volume fraction change with respect to initial

End of injection (50 years)

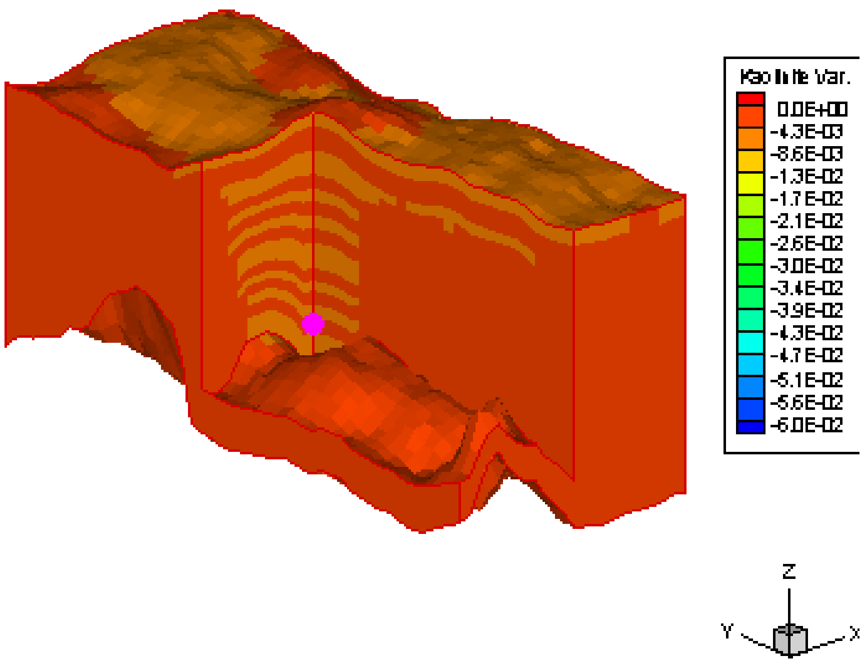

End of storage (1000 years)

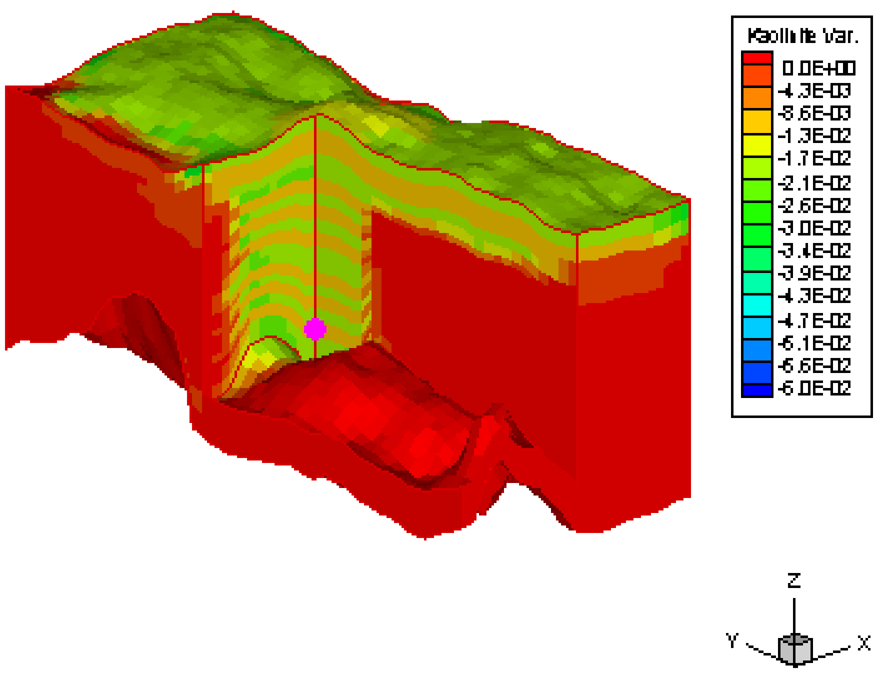

Illite volume fraction change with respect to initial

End of injection (50 years)

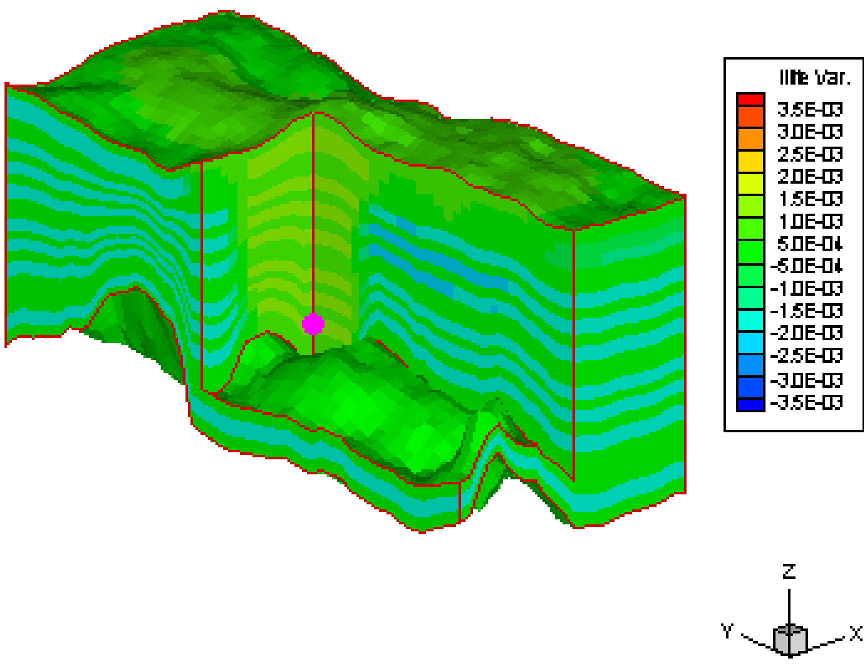

End of storage (1000 years)

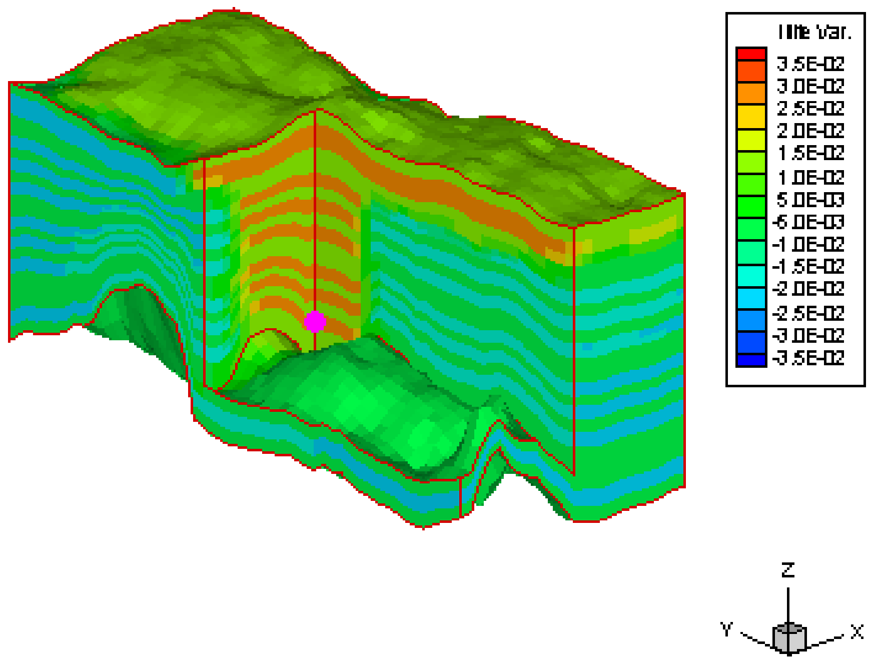

Alumino-silicates mineral behavior

k-feldspar + kaolinite + Mg^{2+} = quartz + illite + H_2O

- during CO_2 injection:
  - limited illite precipitation by Mg^{2+} availability and faster precipitations (dolomite, k-feldspar)
- during CO_2 storage:
  - larger illite precipitation due to mineral dissolutions (dolomite, k-feldspar, kaolinite)

Porosity changes with respect to initial

End of injection (50 years)

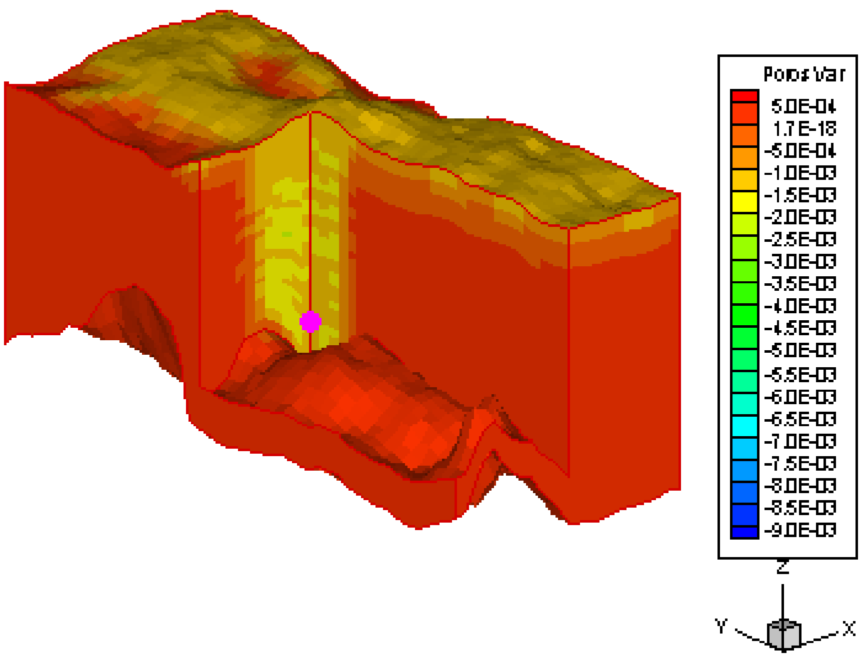

End of storage (1000 years)

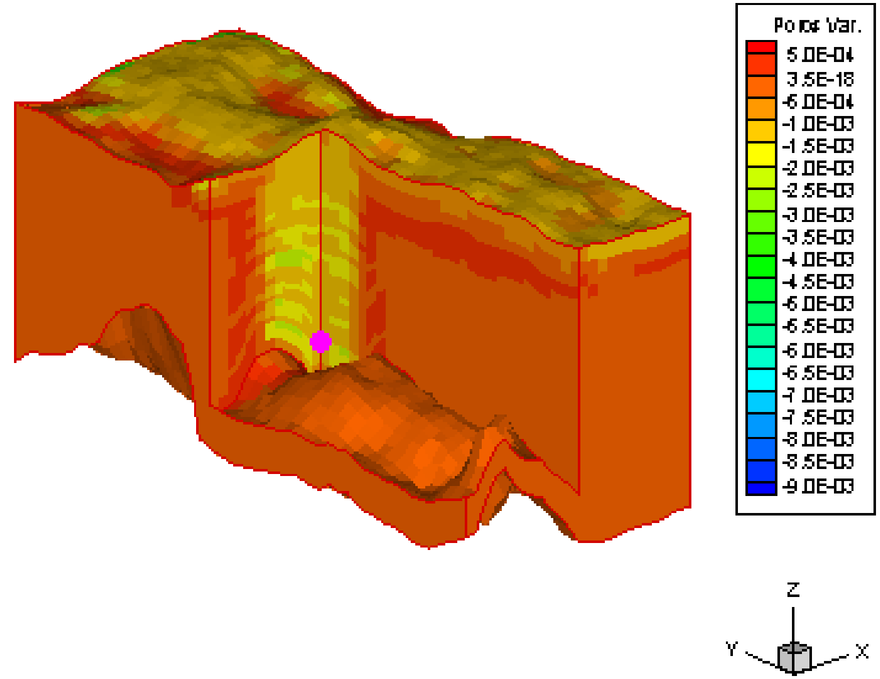

Permeability changes with respect to initial

End of injection (50 years)

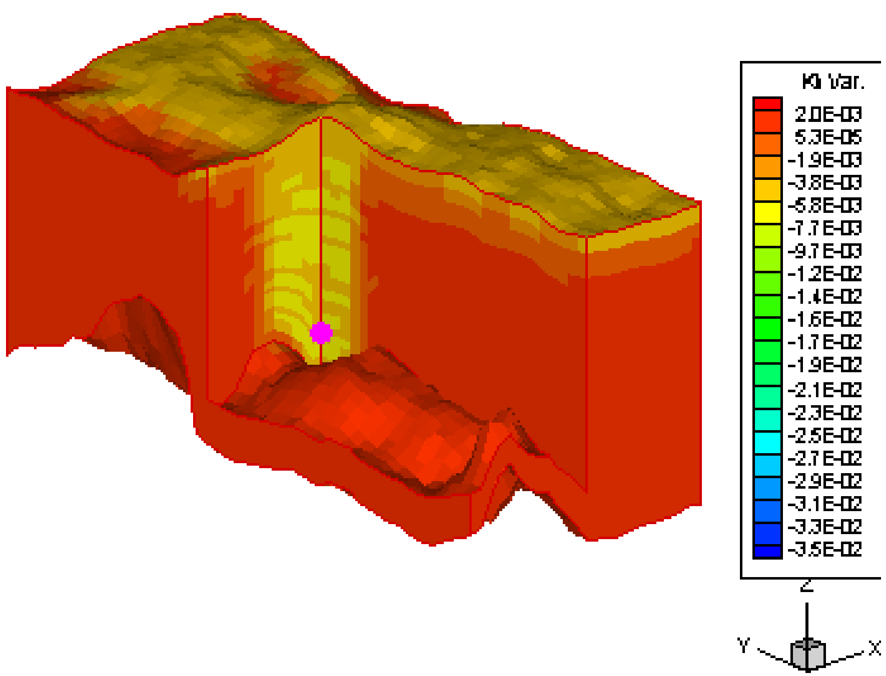

End of storage (1000 years)

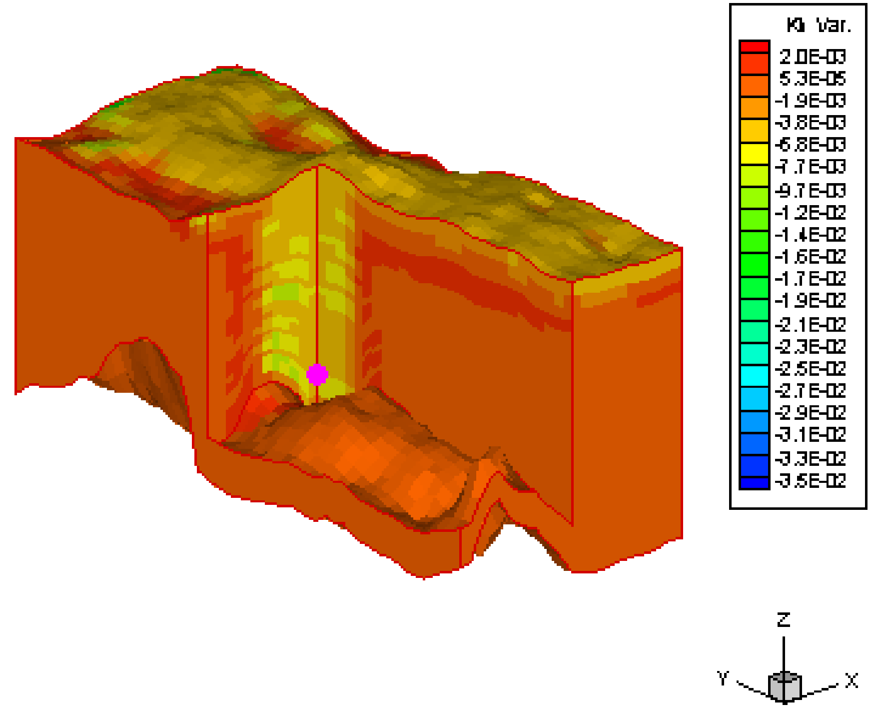

Petrophysical behavior

- limited impact of mineral changes on petrophysical properties (K-ϕ)
  - a slight porosity decrease ($\approx 10^{-3}$ p.u.)
  - a slight permeability decrease (< 1mD)
  - local heterogeneity enhancement due to non-uniform carbonate reactions between sand and shale layers

CO_2 geological trapping

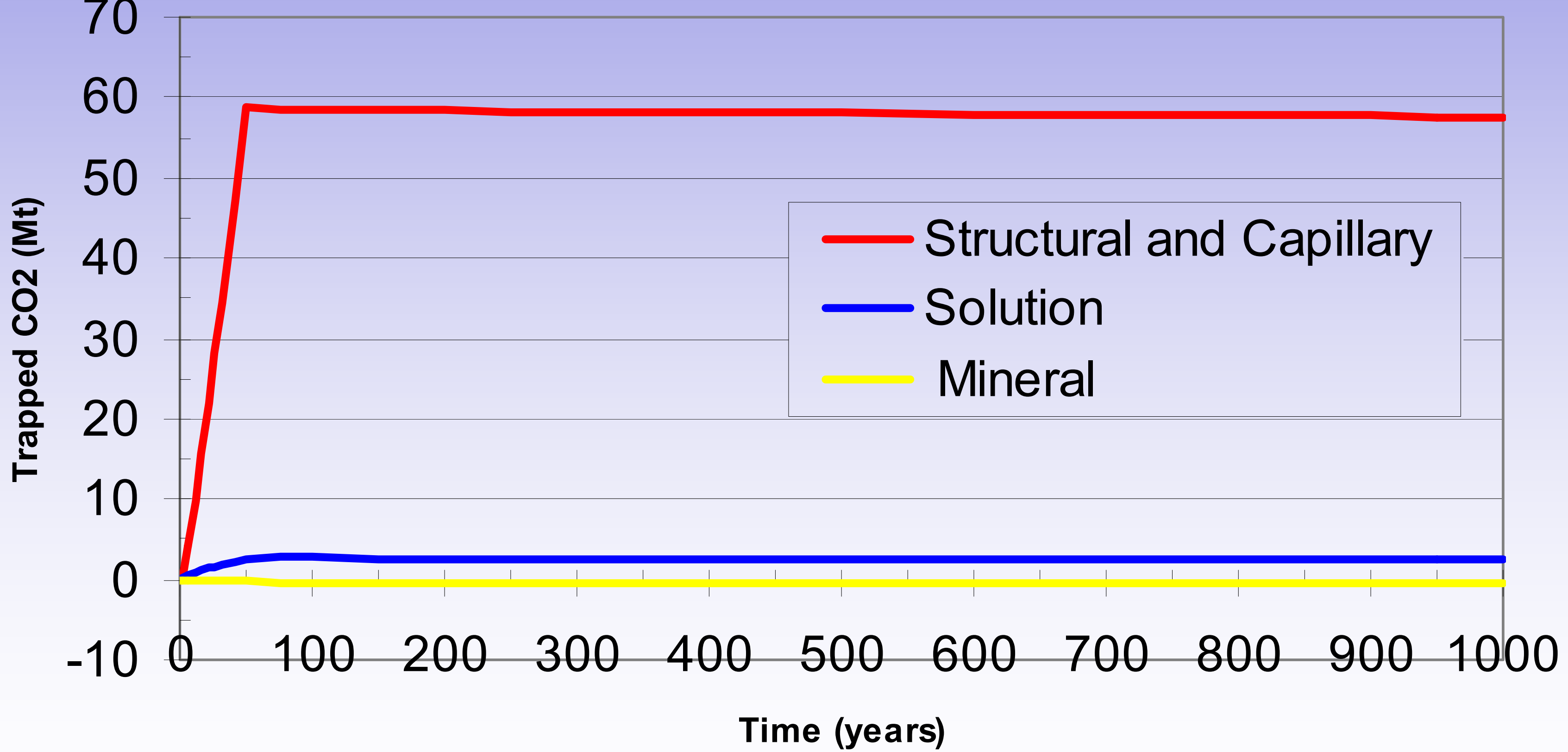

Conclusions

– An efficient coupling approach is implemented to model reactive transport over CO_2 geological storage.
– The sequential implicit algorithm of COORES induces a **CPU time overhead of about 65%** for the reactive transport modeled (7 minerals, 16 aqueous species and 8 chemical elements) with respect to the two-phase flow (37500 grid blocks).
– Different characteristic times between carbonate (calcite and dolomite) and alumino-silicates minerals (illite, kaolinite, k-feldspar) induce competing fronts in the different rock-types of the model (sand and shale)
– The mineral changes have a limited influence on petrophysical properties and flow given their initial values